

An Overview of Infrasound Propagation

R. Waxler¹

National Center for Physical Acoustics
University of Mississippi, United States

ABSTRACT

Acoustic signals from large explosions can be detected at enormous distances from the explosion itself. Although much of the acoustic energy is in the infrasonic band signals are audible many hundreds of kilometers away. An overview of very long range propagation, for both infrasonic and low frequency audible sound will be presented. The significant layers of the atmosphere will be discussed as well as seasonal variations. The role of non-linear propagation in signal audibility will be presented. Results from numerical modeling and data from ground truth experiments will be presented.

Keywords: Infrasound, Propagation, Explosive Transients

1. INTRODUCTION

Infrasound is loosely defined to be sound at frequencies too low to be heard by humans, often quoted as being 20 Hz or less[1, 2]. A distinction is also often drawn between disturbances that are acoustic in that they propagate through compression and rarefaction and disturbances that are buoyant in nature. Buoyant effects are found, roughly, at frequencies of 0.05 Hz or less. Of course the lines between audible and inaudible and acoustic and buoyant are not precisely defined. There is a significant overlap between low frequency audible sound and high frequency infrasound. Similarly, there is a broad band in which a distinction cannot be drawn between buoyant and acoustic and in which signals propagate as coupled acousto-bouyancy waves.

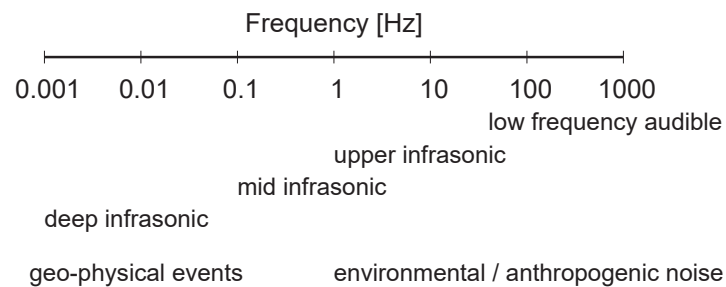


Figure 1. Decomposition of sound fields into frequency bands types.

In Fig.1 frequency bands are labeled and overlaps are indicated. Signals in the band labeled as deep infrasonic are actually coupled acousto-bouyancy waves. These can be generated, for example, as lee waves over mountains, signals from large convective storms or by meteors exploding in the middle atmosphere. The mid-infrasonic band is the most studied. This is the band containing signals generated by moderate sized nuclear explosions, large chemical explosions, as well as by geophysical sources such as volcanoes, the aurora borealis and the ubiquitous microbarom signal generated by colliding ocean waves[3, 4].

Infrasonic signals are global in nature and are routinely detected at enormous distances, from hundreds to thousands of kilometers, from the source. There are several reasons for this. One is that attenuation is small at infrasonic frequencies. Another is that temperature gradients and wind jets provide ducts in which sound can propagate efficiently. Equally significant is that low frequency signals tend to be generated by large or violent events which produce very large signals.

¹email: rwax@olemiss.edu

Our primary concern here will be signals from large chemical explosions, on the order of 100 tons of TNT. The peak frequency of the signals from such explosions is on the order of 0.5 Hz; however, due to the rapid onset of the pressure wave from a blast, the spectrum from a large explosion is quite asymmetrical and has a long high frequency tail. Based on linear propagation theory, the higher frequency components of an explosive signal should attenuate while propagating, leaving only the infrasonic component at long ranges. Contrary to this expectation signals from large explosions are audible hundreds of kilometers away.

2. INFRASOUND PROPAGATION

As always, the acoustic approximation to the equations of fluid mechanics is obtained by expanding about some quiescent atmospheric state. In the simplest approximation the atmosphere is stratified: mean temperature, pressure, density and entropy; T_0 , P_0 , ρ_0 and S_0 ; depend only on altitude z . The mean flow or wind,

$$\mathbf{v}_0 = \begin{pmatrix} \mathbf{v}_{0,H} \\ 0 \end{pmatrix} = \begin{pmatrix} u \\ v \end{pmatrix} \quad (1)$$

where the subscript H indicates projection on the horizontal plane and u and v are the standard atmospheric science notation for longitudinal and meridional wind speed respectively, has no vertical component and the horizontal components depend only on z , but are otherwise unconstrained. In a stratified, adiabatic atmosphere with equation of state given by the ideal gas law $P_0 = \rho_0 RT_0$ the mean mean state can be specified by the temperature alone. Hydrostatic equilibrium implies that

$$P_0(z) = P_0(0)e^{-\frac{g}{R} \int_0^z \frac{1}{T_0(z')} dz'} \quad (2)$$

and mean density and entropy can then be inferred from the thermodynamic relations. In the approximation that buoyancy is insignificant and that vertical wind shear is small on the scale of a wavelength one has the wave equation

$$\left[\nabla_H^2 + \rho_0 \frac{\partial}{\partial z} \left(\frac{1}{\rho_0} \frac{\partial}{\partial z} \right) - \frac{1}{c^2} \left(\frac{\partial}{\partial t} + \mathbf{v}_{0,H} \cdot \nabla_H \right)^2 \right] p_A(\mathbf{x}_H, z, t) = 0. \quad (3)$$

This equation is frequently solved in the frequency domain an the planar approximation in which propagation is limited to a vertical plane and components of the wind transverse to that plane are ignored. In addition, for sufficiently shallow propagation angles and sufficiently small wind speed the effective sound speed approximation[5], in which the wind is included in the sound speed by adding the horizontal wind speed component parallel to the propagation direction to the sound speed, can be used.

2.1 The Atmospheric State

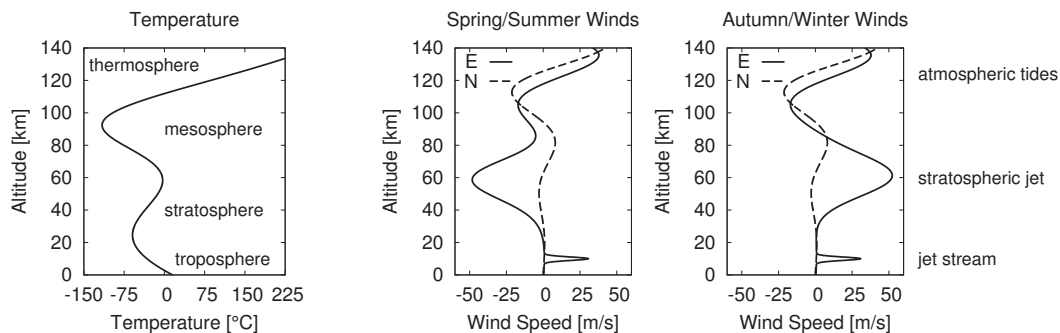


Figure 2: Illustration of the typical atmospheric profile in the northern hemisphere, the primary layers of the atmosphere, and their seasonal variation.

In Fig.2 an illustration of typical temperature and wind jet profiles is shown. The temperature maximum at the top of the stratosphere (known as the stratopause) and the steep increase in temperature in the lower thermosphere produces two sound channels. The typical winds are also shown. The jet stream, at about

about 10 kilometers altitude, is always predominantly eastward flowing with speed depending on latitude and season. The stratospheric jet, at about 50 or 60 kilometers (known also as the circumpolar vortex) depends on season, flowing typically, in the northern hemisphere, to the west in spring and summer and to the east in fall and winter.

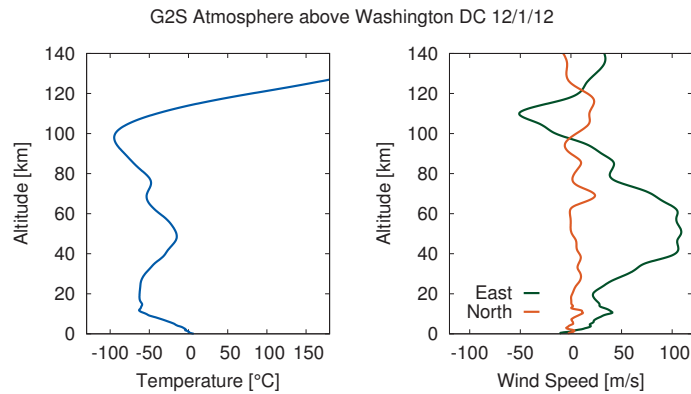


Figure 3: Atmospheric profile above Washington, DC at December 12, 2012; from the G2S model.

In Fig.3 the atmospheric specification above Washington, DC from December 12, 2012, during the six hour period centered at 0600 UTC is shown. The specification is from the US Navy Research Laboratory Ground to Space (G2S) model (see the discussion in Ref.[6] for references and a description of the G2S model). Note the broad eastward flowing stratospheric jet and narrower jet stream. It is to be noted that structure in the atmospheric boundary layer can influence the propagation by providing a ground wave, but any such structure is not seen on the scale of these figures.

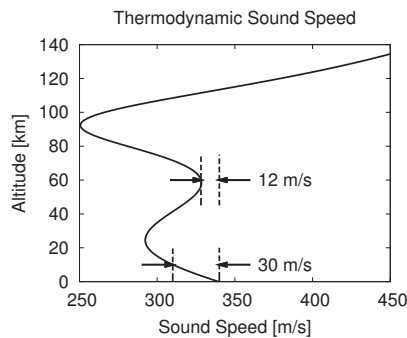


Figure 4: The ducts provided by the thermodynamic sound-speed alone. The temperature maximum at the top of the stratosphere is insufficient on its own to provide a ground duct.

For ground to ground propagation, the ducts in the atmosphere are often poorly formed, borderline ducts that just barely return sound to the ground. The typical situation is illustrated in Fig.4 in which it is shown that the temperature maximum at the stratopause is, except at very cold latitudes, insufficient to return sound to the ground and requires the addition of wind to form a robust channel. Because of this the stratospheric jet is critical for long range infrasound detection. In the example shown in Fig.4 the component of the stratospheric jet in the direction of propagation must be larger than 12 m/s.

Sound can also be ducted by the jet stream; however, due to the steep decrease in the thermodynamic sound-speed in the troposphere the jet stream must be large enough to overcome the resulting upward refraction. In the example shown in Fig.4 the jet stream must be at least 30 m/s.

In Fig.5 the easterly and northerly components of the wind speed, as determined by G2S above the Sinai desert, is shown at 10 and 50 km altitude as a function of time. One sees the following seasonal trends: during the spring and summer months there is a stable westward flowing stratospheric jet. During the Fall and winter months the stratospheric jet flows predominantly to the east, but is not stable. The instabilities are a consequence of what are known as sudden stratospheric warmings (SSWs). There is a persistent eastward flowing jet stream which becomes stronger in the winter and weaker in the summer. The northerly components of

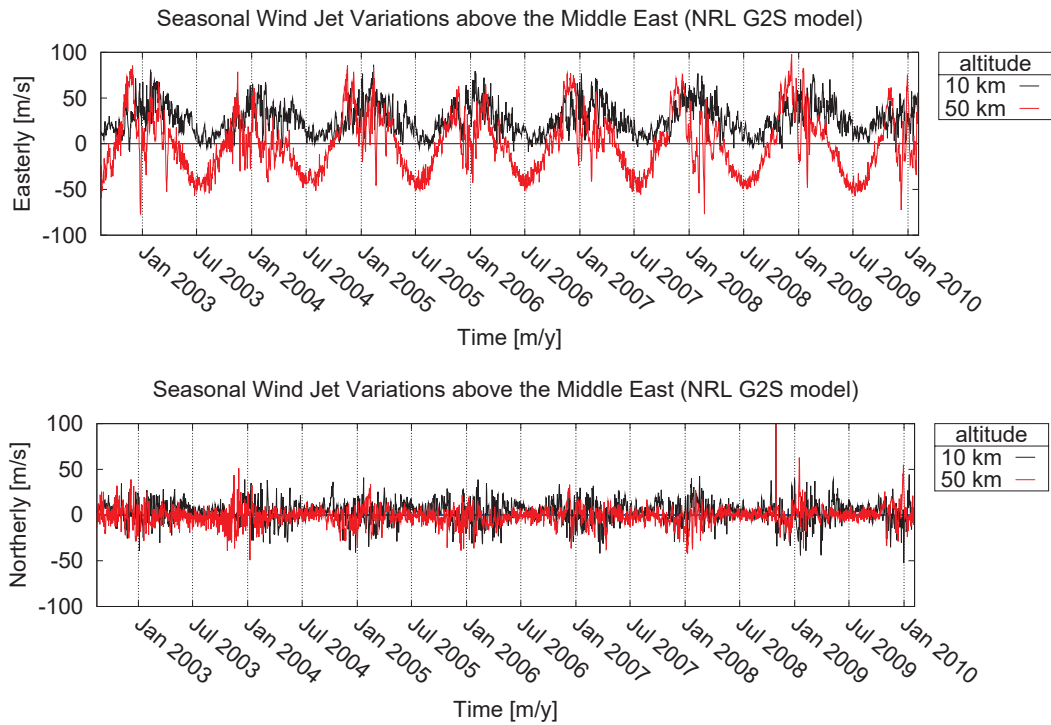


Figure 5: Longitudinal and meridional wind speeds at 50 and 10 kilometers altitude over six years.

the wind are less significant than the easterly, but they do vary over time meaning that any ducts formed by these winds remain predominantly east or west but do have varying north-south components. Except during the periods of equinox, around October and March, the stratospheric jet is sufficient to provide longitudinal ducting. The jet stream, in this region, produces significant ducting in winters, but not in summers.

2.2 Mean Density and Attenuation

The density of the atmosphere decreases dramatically, essentially exponentially, with increasing altitude. This has two significant consequences [6]: attenuation increases dramatically with altitude as does the non-linearity of the sound propagation.

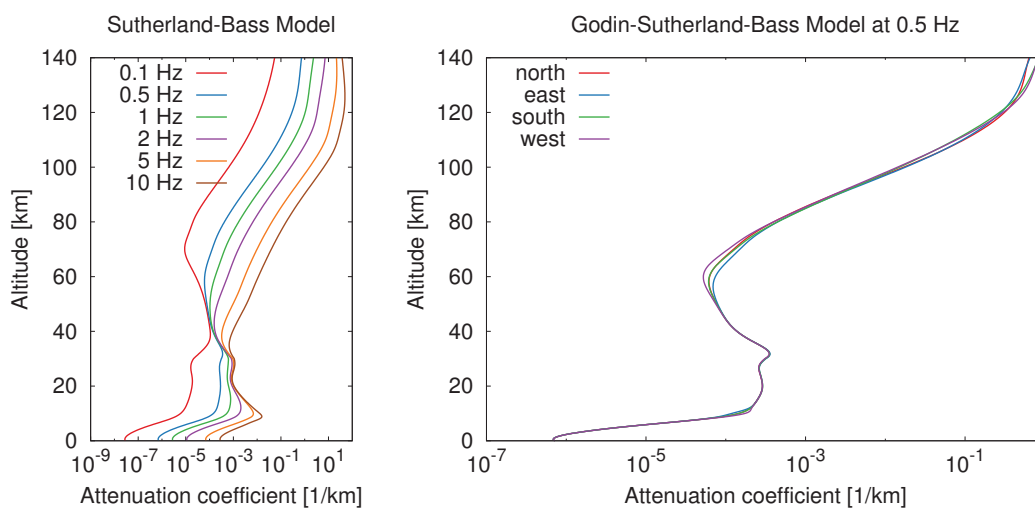


Figure 6. The Sutherland-Bass attenuation model with Godin’s wind speed improvement.

In Fig.6 on the left the Bass-Sutherland [7] attenuation model is shown. We note that humidity is insignificant above the atmospheric boundary layer and so has been set to zero. Note that attenuation increases

dramatically with altitude as well as with frequency. This is a direct consequence of the decrease in atmospheric density. In the right panel an improvement introduced recently by Godin [8] is shown. Godin has shown that for acoustic propagation the influence of the wind is taken into account by replacing the angular frequency ω in the attenuation coefficient with $\omega - \mathbf{k} \cdot \mathbf{v}_0$ where \mathbf{k} is the wave vector. Note that attenuation is enhanced downwind and diminished upwind.

2.3 Typical Propagation Paths

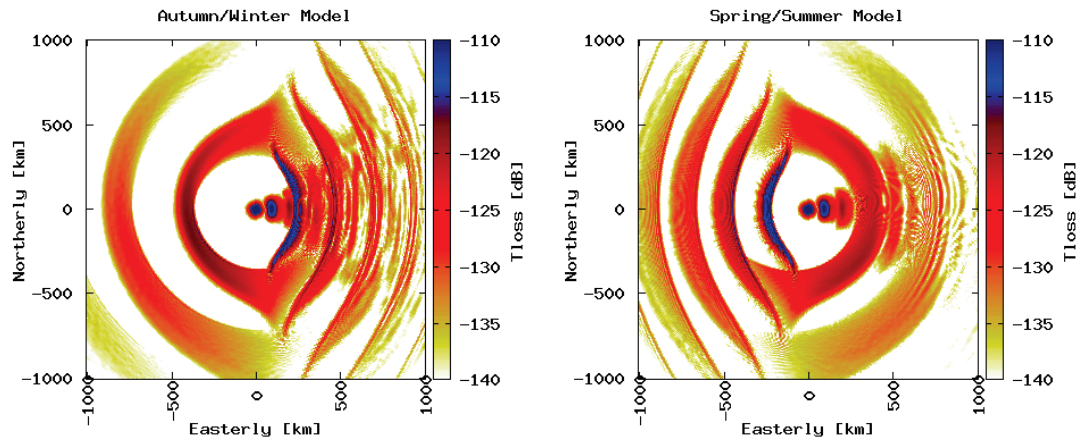


Figure 7: Insonification maps at 0.5 Hz for ground to ground full wave propagation with an eastward flowing and westward flowing stratospheric jet.

In Fig.7 Full wave ground to ground transmission loss models are shown for the spring/summer and autumn/winter models shown in Fig.2. The model modal expansion. Attenuation has not been included so that the returns from the thermosphere are visible. Note the severe anisotropy of the propagation which results from the payoff between downwind versus upwind propagation. Tropospheric ducting is seen to the east as ground bounces about 50 kilometers apart. The stratospheric returns are seen to the east in the autumn/winter model and to the west in the spring/summer model as ground bounces about 240 kilometers apart. Thermospheric returns are seen as rings at about 300 and 600 kilometers range.

In Fig.8 effective sound speeds for various typical atmospheric scenarios are shown next to the ray paths in those effective sound speed profiles. The transmission loss is calculated along the paths by solving the sub-leading order of the geometrical acoustics approximation, the so-called transport equation. The tropospheric, stratospheric and thermospheric phases are seen clearly. Typically, tropospheric paths are characterized by shallow launch angles, up to a few degrees, stratospheric paths by angles up to about 20 degrees or so and thermospheric paths by angles up to 40 or 50 degrees. Long range infrasound propagation, in contrast to boundary layer or ocean propagation, involves quite steep angles.

In all of these simulations if attenuation were included no thermospheric returns would be predicted, as the signals would attenuate so greatly up in the thermosphere before returning to Earth. The acoustic pressure scales with the square root of the density, and the lower amplitudes at high altitudes is a consequence of the decreasing density (this factor is often divided out, but has not been done so here).

In the absence of a tropospheric wind jet waveforms in the stratospheric duct have a canonical form: they arrive in pairs known as the fast and slow arrivals [9]. In the presence of a jet stream, and at infrasonic frequencies the thickness of the jet stream can be on the order of an acoustic wavelength, meaning that the geometrical acoustics approximation is not valid. Energy can leak out of the tropospheric duct formed by the jet stream and then return to Earth as stratospheric arrivals.

A significant issue with infrasound propagation, particularly in a stratospheric duct, are small scale atmospheric fluctuation, presumed to be produced by buoyancy waves overlaid on the mean atmospheric state [10]. Because the atmospheric ducts, for ground to ground propagation, are often marginal, the sound speed fluctuations associated with atmospheric fine structure can have a large influence on signal propagation. Indeed, as opposed to ocean or boundary layer propagation, the presence of such fine scale can produce a duct for ground to ground propagation where the mean effective sound speed is not sufficient to return signal to

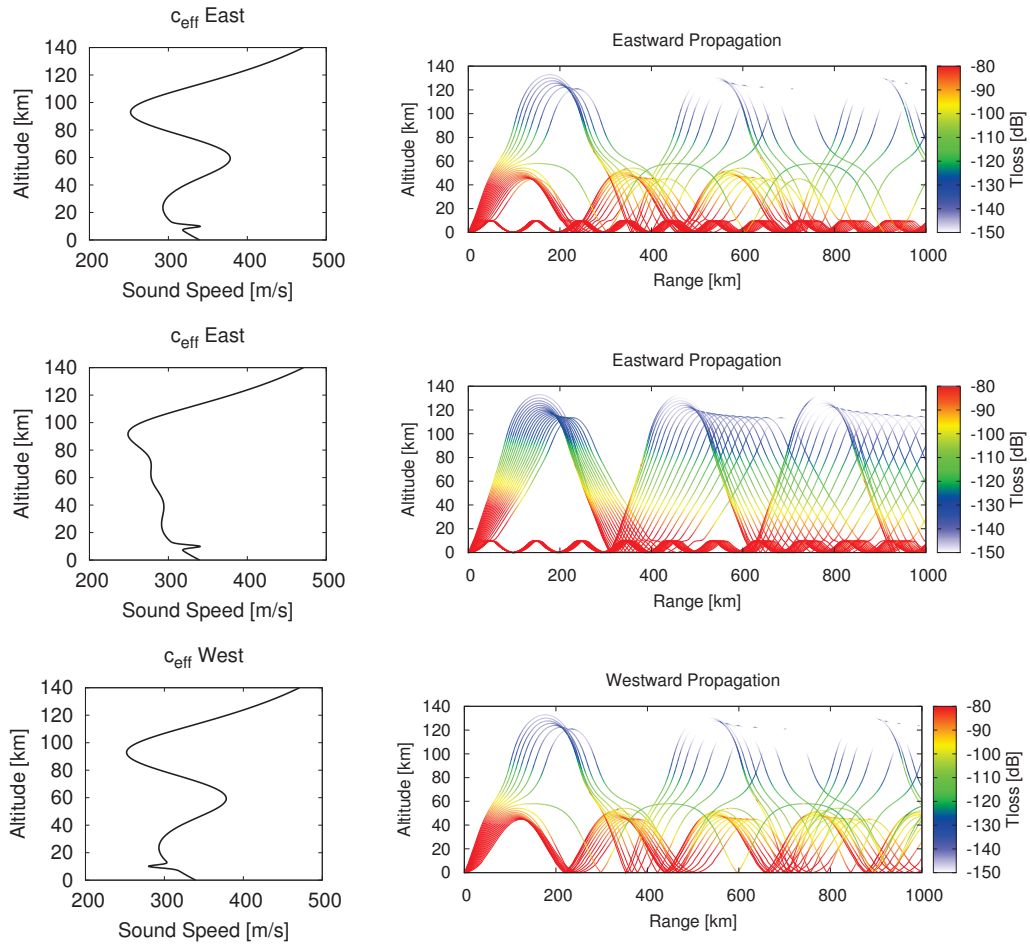


Figure 8: The ray paths and transmission loss along them for propagation in the ducts provided by the wind and sound-speed. The effective sound-speeds are shown to the left of the ray paths. The panels show eastward propagation with an eastward flowing stratospheric jet, eastward propagation with a westward flowing stratospheric jet and westward propagation with a westward flowing stratospheric jet.

the Earth. In this sense fine structure from buoyancy waves can be significant at leading order, rather than as a perturbation on the waveform.

2.4 Linear versus Non-linear Propagation

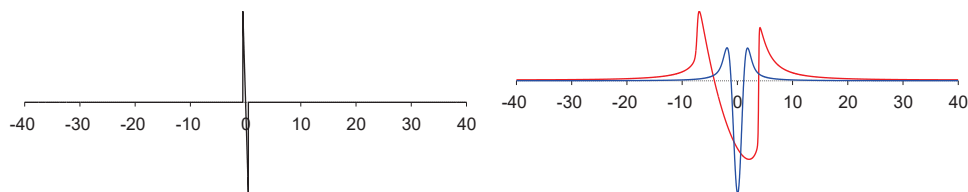


Figure 9: An impulsive waveform 1 km from the source, on the left, and after being propagated according to the non-linear ray theory model through a thermospheric path to a range of 350 km from the source. The result of linear propagation is included for reference.

Because the non-linear corrections to the equations of acoustic propagation become larger with decreasing mean density non-linear propagation becomes more significant the higher in the atmosphere a signal travels. For a transient signal there are primarily two forms non-linear distortion takes (see eg [6]). On the one hand, waveforms steepen and form shocks. On the other, waveforms lengthen and develop longer and longer periods. Waveform steepening is associated with the generation of higher frequency harmonics while period lengthening with the generation of lower frequencies. It is to be emphasized that the high frequency and low

frequency generation produces frequency components that were not present in the source, but are generated along the propagation path by interaction with the atmosphere.

In Fig.9 the result of non-linear propagation through the thermosphere is illustrated with output from a non-linear ray theory model in red [6] compared to that of linear propagation modeling in blue. On the left the waveform at 1 kilometer is shown and on the right the result of propagating that waveform along a thermospheric path out to a range of 350 kilometers is shown. The path passes through a caustic upon which the signal undergoes a phase change of 90 degrees, resulting in a U-wave rather than the initial N-wave-like form. More significantly, the period of the signal increases from about 2 seconds to almost 20 seconds. In addition, the signal at 350 kilometers shows very steep onsets compared to the predictions of linear propagation as a result of high frequency generation associated with waveform steepening.

3. GROUND TRUTH EXPERIMENTS

3.1 Sayarim

In January, 2011, the Comprehensive Nuclear Test Ban Treaty Organization (CTBTO) sponsored an extensive field test centered around the Sayarim test range in the Negev desert in Israel. The Israeli Defense Forces and the Geophysical Institute of Israel designed and detonated a charge of about 100 tons of chemical explosive as a nuclear weapon surrogate for purposes of collecting data and testing the CTBTO verification regime [11]. Instrumentation both in the near and far field was deployed. In Fig.10 a map of the far field deployment is shown. The signal was detected as far as Mongolia over 6000 kilometers away.

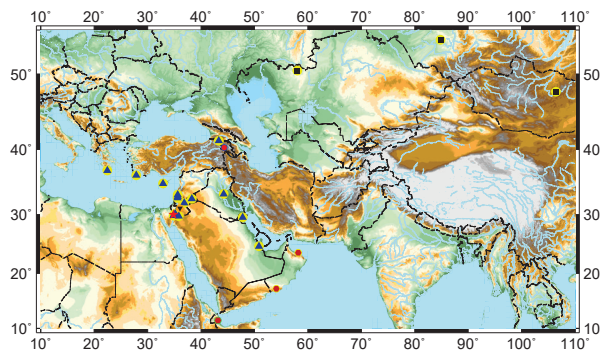


Figure 10. Map of the 2011 Sayarim calibration test deployment.

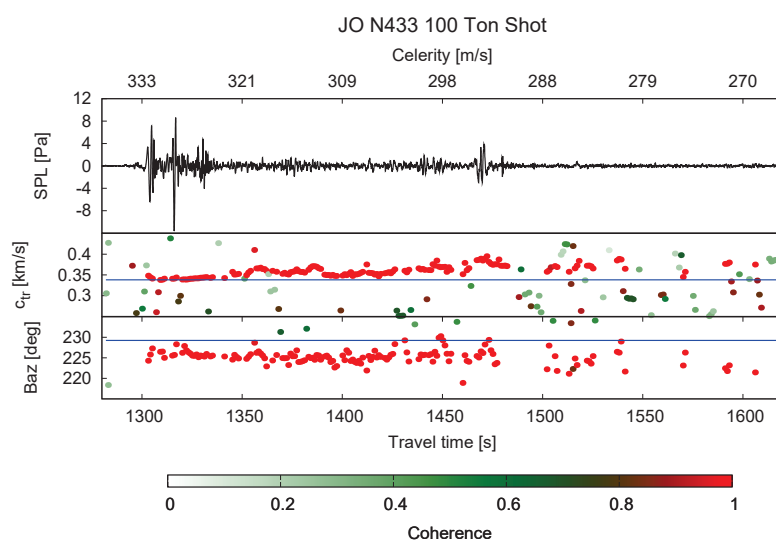


Figure 11: Signal from Sayarim 2011 received on an array in Jordan about 433 kilometers to the north-east of the explosion.

As expected based on climatology of the atmosphere, detections were made exclusively to the east of the

explosion. As there was a very strong jet stream there were far reaching tropospheric returns. In Fig.11 the signal received on an array of infrasound sensors in Jordan, about 433 kilometers to the north-east is shown along with results, apparent back azimuth and array velocity, of array processing. The first three phases are tropospheric, followed by scattered sound and ending with a stratospheric phase. It is to be noted that researchers tending the array during the experiment report that the signal was audible.

3.2 Humming Roadrunner

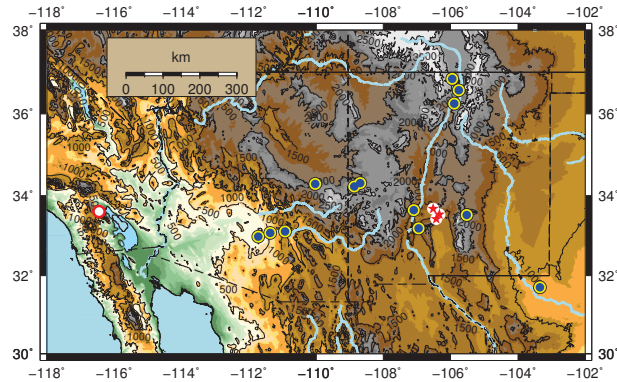


Figure 12. Humming Roadrunner exercise: far field deployment.

In August 2012 the US Department of Defense detonated 6 chemical explosive charges ranging from 10 to 50 tons of TNT equivalent in the desert of New Mexico. Infrasound arrays were deployed north, south and west to capture the signals. All six signals were detected out to California about 1000 kilometers to the west.

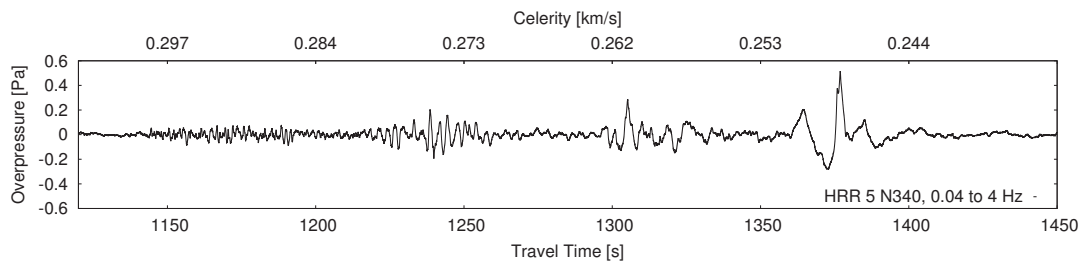


Figure 13. Signal received from a 50 ton shot 340 kilometers to the north.

In Fig.13 an example detection is shown. It is the signal from a 50 ton (TNT equivalent) explosion received about 340 kilometers to the north of the explosion. The sequence of phases are believed to be stratospheric, stratospheric, mesospheric and thermospheric. Note that the frequency content of the phases decreases steadily until the thermospheric phase has a dominant period of almost 20 seconds. The two stratospheric and mesospheric phases are not predicted by G2S and are thought to be the result of refraction by winds associated with buoyancy waves.

4. CONCLUSIONS AND DISCUSSION

Signals from large explosions have been reported to be audible at great distances from the explosion itself. This seems to be at odds with results of linear propagation modeling which shows that audible frequencies attenuate to undetectable levels hundreds of kilometers from the source. In addition, linear propagation modeling predicts that signal returns along thermospheric paths would also attenuate to undetectable levels, contrary to experience in which thermospheric returns are often detected. The role of non-linearity appears to be critical in explaining these discrepancies. Waveform shocking in the stratosphere appears to be responsible for high frequency generation that allows signals to be audible hundreds of kilometers from the source. Signals which propagate into the thermosphere before returning to Earth undergo severe period lengthening. The causes the frequency content of the signal to decrease dramatically, preventing the signal from being attenuated by the severe attenuation in the thermosphere.

REFERENCES

- [1] A. Bedard and T. Georges. Atmospheric infrasound. *ACOUSTICS AUSTRALIA*, 28(2):47–52, 2000.
- [2] A. Le Pichon, E. Blanc, and A. Hauchecorne, editors. *Infrasound Monitoring for Atmospheric Studies*. Springer, New York, 2010.
- [3] L. M. Brekhovskikh, V. V. Goncharov, V. M. Kurtepov, and K. A. Naugol'nykh. The radiation of infrasound into the atmosphere by surface waves in the ocean. *Izv. Atmospheric and Oceanic Physics*, 9(9):pp. 899 to 907, 1973.
- [4] R. Waxler and K. E. Gilbert. The radiation of microbaroms by ocean surface waves. *J. Acoust. Soc. Am.*, 119(5):pp. 2651 to 2664, 2006.
- [5] O. Godin. An effective quiescent medium for sound propagating through an inhomogeneous, moving fluid. *J. Acoust. Soc. Am.*, 2002.
- [6] J. Lonzaga, R. Waxler, J. Assink, and C. Talmadge. Modelling waveforms of infrasound arrivals from impulsive sources using weakly non-linear ray theory. *Geophys. J. Int.*, 2015.
- [7] L. C. Sutherland and H. E. Bass. Atmospheric absorption in the atmosphere up to 160 km. *J. Acoust. Soc. Am.*, 99(3):pp. 1012 to 1032, 2004.
- [8] O. Godin. Dissipation of acoustic gravity waves: An asymptotic approach. *J. Acoust. Soc. Am.*, 2014.
- [9] R. Waxler, L. G. Evers, J. Assink, and P. Blom. The stratospheric arrival pair in infrasound propagation. *The Journal of the Acoustical Society of America*, 137(4):1846–1856, 2015.
- [10] J.M. Lalande and R. Waxler. The interaction between infrasonic waves and gravity wave perturbations: application to observations using uttr rocket motor fuel elimination events. *Journal of Geophysical Research: Atmospheres*, pages n/a–n/a, 2016. 2015JD024527.
- [11] David Fee, Roger Waxler, Jelle Assink, Yefim Gitterman, Jeffrey Given, John Coyne, Pierrick Mialle, Milton Garces, Douglas Drob, Dan Kleinert, et al. Overview of the 2009 and 2011 sayarim infrasound calibration experiments. *Journal of Geophysical Research: Atmospheres*, 118(12):6122–6143, 2013.